Description of SU(3) *s*-wave and *p*-wave baryons

Mikito Furuichi and Kiyotaka Shimizu*
Department of Physics, Sophia University, Chiyoda-ku, Tokyo 102-8554, Japan

Sachiko Takeuchi
Japan College of Social Work, Kiyose, Tokyo 204-8555, Japan

(Received 27 May 2002; revised manuscript received 27 December 2002; published 4 September 2003)

We investigate the structure of the SU(3) octet and decuplet baryons employing a constituent chiral quark model. We solve the ground and *s*- and *p*-wave excited states of the three-quark system with many range Gaussian bases. This method, which we employ here, has been shown to work quite nicely to describe the structure of the SU(3) *s*-wave baryons. In this work, we extend our research to the SU(3) *p*-wave baryons including the tensor term. It is found that the mass differences between positive and negative parity states are well reproduced. It is also found that the pseudoscalar (ps) meson exchange potential plays a very important role to lower the mass of the nucleon resonance $N^*(1440)$ (Roper). We also discuss how the semirelativistic approach works in the chiral quark model and how to treat the potential terms consistently in the semirelativistic approach.

DOI: 10.1103/PhysRevC.68.034001 PACS number(s): 12.39.Jh, 12.39.Pn, 14.20.−c, 12.40.Yx

I. INTRODUCTION

There have been many studies on the SU(3) octet and decuplet *s*- and *p*-wave baryons in terms of the constituent quark model [1]. Due to the breaking of the flavor-spin symmetry, the mass spectra of the SU(3) octet and decuplet baryons are very complicated. The investigation of this complicated baryon mass spectra using the constituent quark model is one of the fundamental researches in understanding QCD in the low energy nonperturbative regime. There are several constituent quark models employing residual interactions which are suggested by a study of low energy QCD. Isgur and Karl [2] have introduced a quark model that employs one gluon exchange potential (OGEP) [3]. The color magnetic part of OGEP, which has $\boldsymbol{\sigma}_i \cdot \boldsymbol{\sigma}_j v_0$ dependence, becomes $-3v_0$ for the octet baryons, while it becomes $3v_0$ for the decuplet baryons that contain only pairs with $S=1$. This has been believed to produce the mass difference between the nucleon and Δ and generally the mass difference between octet and decuplet baryons [2].

Although their simple nonrelativistic quark model employing the harmonic oscillator-type confinement potential gives a good qualitative description of octet and decuplet baryons including *p*-wave states, their quark model has some defects in reproducing some other observed baryon spectra. One of the famous defects is a failure of explaining a state of the first positive parity resonance of the nucleon $N^*(1440)$, the so-called ''Roper resonance.'' There they had to introduce an unknown term to lower the mass of the Roper resonance. The mass ordering of the positive and negative parity excited nucleons has been a famous puzzle not only for the traditional constituent quark model but also for recent other quark models. For example, according to the recent calculation of the baryon spectra in quenched lattice QCD [4], the indication of the positive parity excited state that may correspond to the state of the Roper resonance has been confirmed. However, they could not succeed in reproducing the right mass ordering.

Recently the so-called chiral quark model claims that the mass difference between the excited baryons can be explained by the pseudoscalar (ps) meson exchange potential [5]. This argument is based on the spontaneous chiral symmetry breaking, which changes the current quark mass to the constituent quark mass and is accompanied by an appearance of pions as the Goldstone bosons and its chiral partner sigma (σ) meson. In the SU(3) case, the SU(3) octet ps mesons as the Goldstone bosons and the chiral partner σ meson appear due to the spontaneous chiral symmetry breaking. This model has been employed for the description of single baryons [6] with the relativistic treatment of the kinetic energy term [7].

The ps meson exchange potential has a flavor-spin dependence that has the form $-\boldsymbol{f}_i \cdot \boldsymbol{f}_j \boldsymbol{\sigma}_i \cdot \boldsymbol{\sigma}_j v_0$, where $\boldsymbol{f}$ is the flavor SU(3) generators. Employing a similar argument as before, the ps meson exchange potential can also produce the mass difference between octet and decuplet baryons. In addition, this flavor-spin dependent term becomes $-14v_0$ for the flavor-spin SU(6) $[3]_{fs}$ symmetry state, while it becomes $-2v_0$ for the flavor-spin SU(6) $[21]_{fs}$ symmetry state for the octet baryons with spin$=\frac{1}{2}$. Therefore the flavor-spin dependent term is expected to reproduce the correct ordering of the Roper and the *p*-wave nucleon resonances. This is one of the reasons why the chiral quark model is thought to be a fascinating quark model [8], even though there seems to remain problems which should be clarified.

In order to solve the three-constituent quark system, we employ the diquarklike cluster model that has been employed before [9,10]. The characteristic feature of the diquarklike model is that quark pairs can behave differently in accordance with their spin and flavor symmetries. Due to the spin dependence of the short range part of the ps meson exchange potential, the size of the $S=0$ quark pairs becomes much smaller than that of the spin $S=1$ pairs. We found this

*Email address: k-simizu@sophia.ac.jp

difference in their behavior plays an essential role to gain the mass difference between octet and decuplet baryons. This is one of the reasons why our simple variational model works quite nicely to describe *s*-wave baryons in Refs. [9,10]. We must note that our model does not assume the diquark-quark configuration. We solve a three-body problem. Since the solution shows the diquark correlations, which is in effect similar to a diquark picture of the octet baryons [11,12], we call this model ''diquarklike model.'' Here we extend this method to the study of the negative parity *p*-wave baryons including the tensor term.

Because of the strong short range attraction due to the ps meson exchange potential, we have to treat the short range part very carefully, especially in the semirelativistic approach. As will be shown, the nonrelativistic kinetic energy term suppresses the short range part more strongly than the relativistic one. Therefore the result in the nonrelativistic calculation is not sensitive to the details of the short range attraction. On the other hand, the short range attraction contributes very strongly in the semirelativistic approach. Therefore we must treat the short range part very carefully. For this purpose we have proposed an improved method to solve the variational problem numerically [10].

We also pay attention to the semirelativistic approach itself. The calculation where the kinetic energy is replaced by the relativistic form must incorporate the potential terms which include some relativistic effects. The relativistic kinetic energy form is just a step to the consistent relativistic corrections.

Because of an uncertain nature of the Roper resonance, there remains an open question of whether or not the Roper resonance is a simple radial excitation of the three-quark system [13]. However, it is interesting to look for a model that can reproduce the state of the Roper resonance as the simple three-quark system and to see how it describes the resonance. We first employ the constituent chiral quark model used in Ref. [6] and show that our calculational method reproduces the results given by the stochastic variational method. This indicates that our simple calculational method works very well even in negative parity baryon states and enables us to investigate the roles of each term in the Hamiltonian for the SU(3) baryons in the same way as in Ref. [10]. It is found [6] that the ps meson exchange potential works effectively to lower the mass of the Roper resonance more strongly than the *p*-wave states. In other words, the strong attraction due to the pion is needed to shift the mass of the Roper resonance, although the attractive contribution seems too large in their approach [6]. Moreover, in order to obtain the correct nucleon mass, a constant attraction has been introduced instead of including an attractive short range potential due to the σ meson, which is a chiral partner of the octet ps mesons. Furthermore the repulsive potential due to the SU(3) singlet ps meson η' exchange has been included in their calculation. Omitting the short range attraction and including the short range repulsion are necessary to prevent the system from a collapse due to the strong attractive octet ps meson exchange potential in their semirelativistic approach [6].

In order to understand the chiral model much more deeply, we make two kinds of calculations. First we carry out the calculation employing the nonrelativistic quark model, which can reproduce the mass ordering of the nucleons. As we mentioned in Ref. [10], it may be consistent to employ the nonrelativistic expression of the kinetic energy term when we use the nonrelativistic form of the ps meson exchange potential. The result shows how the nonrelativistic approach can reproduce the mass of the Roper resonance with an enormous pion contributions. Next we propose the semirelativistic quark model, which is stable even if the σ meson exchange potential [14] is included explicitly. Here we take into account the relativistic effects not only on the kinetic energy term but also on the potential terms. The latter effects are expressed as a smaller cutoff parameter, which takes care of the short range behavior of the ps meson exchange potentials.

In this work, we also investigate the effects of the tensor term, which mixes the different spin states and contributes to the mass of each *j* state differently. The mixing due to the tensor term has been studied using symmetry-based quark models [8,17,18]. We will show that the mixing is found to be rather small in our work as compared to their results.

In the following section, we explain a diquarklike cluster model for *p*-wave baryons where the mixing of symmetries other than usual $[21]_o$ are taken into account. This model is based on the diquark picture of the baryon, but the system is completely antisymmetrized under quark exchanges among three-constituent quarks. In Sec. III, we explain the chiral quark models in the semirelativistic or nonrelativistic approach. Then in Sec. IV, we show several formulas that have been frequently used in the quark cluster model [15,16] to calculate the Hamiltonian, normalization and the properties of the pair with the flavor and spin symmetry ($[f]S$). Then in Sec. V, the results employing the various chiral quark models are given. We summarize the results in Sec. VI.

II. DIQUARKLIKE CLUSTER MODEL

A. Wave function

The harmonic oscillator wave function has been frequently employed for the trial function to study the baryon structure [2,15,16]. Instead of using a single range oscillator wave function, a linear combination of several orthogonal bases [19,20] or Gaussian with different ranges has been employed [21]. It is shown that this kind of many-range Gaussian trial wave function works quite nicely for the nucleon and Δ [9]. Therefore, we have employed the following linear combination of many-range Gaussians for the trial wave function of the *s*-wave SU(3) baryons [9,10]:

$$\Phi(\boldsymbol{\rho},\boldsymbol{\lambda})=\mathcal{S}\sum_{i,j,M_f S} C_{ijM_f S}|ij\rangle\left|M_f;\left(S,\frac{1}{2}\right)s\right\rangle, \tag{1}$$

$$|ij\rangle=\left(\frac{1}{\sqrt{\pi}c_i}\right)^{3/2}\left(\frac{1}{\sqrt{\pi}d_j}\right)^{3/2}\exp\left(-\frac{\boldsymbol{\rho}^2}{2c_i^2}-\frac{\boldsymbol{\lambda}^2}{2d_j^2}\right), \tag{2}$$

where $C_{ijM_f S}$ is the expansion coefficients, and $\mathcal{S}$ is a symmetrization operator, which is written as

$$\mathcal{S}=1+2P_{23}=1+2P_{23}^{(o)}P_{23}^{(f\sigma)}, \tag{3}$$

where P_{23} is an exchange operator of the quarks 2 and 3, which is a product of the orbital part $P^{(o)}$ and flavor-spin part $P^{(f\sigma)}$. $|M_f;(S,\frac{1}{2})s\rangle$ is the flavor-spin part. For the ground state octet baryons, M_f is a mixed symmetric state $[21]_s$ or mixed antisymmetric state $[21]_a$, and the first and second quarks couple to spin S and the total spin is $s=\frac{1}{2}$. For the ground state decuplet baryons, the flavor part is $M_f=[3]$ and spin part is also [3], namely, $S=1$ and $s=\frac{3}{2}$. $\boldsymbol{\rho}$ and $\boldsymbol{\lambda}$ are internal coordinates and c_i and d_j are the range parameters. The internal coordinates $\boldsymbol{\rho}$ and $\boldsymbol{\lambda}$ and the center-of-mass coordinate $\boldsymbol{R}$ are taken as

$$\boldsymbol{\rho}=\boldsymbol{r}_1-\boldsymbol{r}_2, \quad \boldsymbol{\lambda}=\frac{\boldsymbol{r}_1+\boldsymbol{r}_2}{2}-\boldsymbol{r}_3, \tag{4}$$

$$\boldsymbol{R}=\frac{m_1\boldsymbol{r}_1+m_2\boldsymbol{r}_2+m_3\boldsymbol{r}_3}{m_1+m_2+m_3}. \tag{5}$$

As seen in Ref. [10], we can define the conjugate momenta $\boldsymbol{p}_\rho$, $\boldsymbol{p}_\lambda$, and $\boldsymbol{P}$, which have a simple relation with the quark momentum.

In this paper, we also employ the following combination of many range Gaussians for *p*-wave baryons:

$$\Phi(\boldsymbol{\rho},\boldsymbol{\lambda})=\mathcal{S}\sum_{i,j,M_fS}C_{ijM_fS}|ij;[o]\rangle\left|M_f;\left(S,\frac{1}{2}\right)s\right\rangle, \tag{6}$$

where $|\ ij;[o]\rangle$ is an orbital part and $[o]$ is its symmetry $[2]$ or $[11]$ under the exchange of quarks 1 and 2.

Because the orbital parts must couple to a flavor-spin parts so that they make a totally symmetric state, two types of the orbital wave functions are taken into account in the following way. When a flavor-spin part is antisymmetric under the exchange of the quarks 1 and 2, such as $|[21]_s;(0,\frac{1}{2})s\rangle$, $|[21]_a;(1,\frac{1}{2})s\rangle$, and $|[111];(1,\frac{1}{2})s\rangle$, orbital part must be also antisymmetric under the same exchange, and we employ the following bases:

$$|ij;[11]\rangle=\sqrt{\frac{2}{3}}\frac{1}{c_i}\left(\frac{1}{\sqrt{\pi}c_i}\right)^{3/2}\left(\frac{1}{\sqrt{\pi}d_j}\right)^{3/2}\times\boldsymbol{\rho}\exp\left(-\frac{\boldsymbol{\rho}^2}{2c_i^2}-\frac{\boldsymbol{\lambda}^2}{2d_j^2}\right). \tag{7}$$

On the other hand, if a flavor-spin part is symmetric under the exchange of quarks 1 and 2, such as $|[21]_a;(0,\frac{1}{2})s\rangle$, $|[21]_s;(1,\frac{1}{2})s\rangle$, $|[3];(1,\frac{1}{2})s\rangle$, and $|[111];(0,\frac{1}{2})s\rangle$, we employ

$$|ij;[2]\rangle=\sqrt{\frac{2}{3}}\frac{1}{d_j}\left(\frac{1}{\sqrt{\pi}c_i}\right)^{3/2}\left(\frac{1}{\sqrt{\pi}d_j}\right)^{3/2}\times\boldsymbol{\lambda}\exp\left(-\frac{\boldsymbol{\rho}^2}{2c_i^2}-\frac{\boldsymbol{\lambda}^2}{2d_j^2}\right). \tag{8}$$

Because the trial wave functions in Eqs. (2), (7), and (8) are given in terms of the internal coordinates only, the center-of-mass motion is already removed although many Gaussians with different ranges can be employed. Note that if the size parameters are $c_i=\sqrt{4/3}\,d_j$, the above trial wave function of the *s* wave, Eq. (1), becomes totally symmetric $[3]_o$ in the orbital space and its flavor-spin part belongs to $[3]_{fs}$ of the flavor-spin SU(6) group.

Similar to the *s*-wave case, the trial wave function of the *p* wave, Eq. (6), becomes $[21]_o$ and its flavor-spin part also belongs to $[21]_{fs}$ when $c_i=\sqrt{4/3}d_j$. So in the case of the octet baryons with $s=\frac{1}{2}$, the trial wave function is written as

$$\begin{aligned}&\frac{1}{\sqrt{4}}\{|[21]_s;(S=1,\tfrac{1}{2})s=\tfrac{1}{2}\rangle-|[21]_a;(S=0,\tfrac{1}{2})s=\tfrac{1}{2}\rangle\}|ij;[2]\rangle\\&-\frac{1}{\sqrt{4}}\{|[21]_s;(S=0,\tfrac{1}{2})s=\tfrac{1}{2}\rangle+|[21]_a;(S=1,\tfrac{1}{2})s=\tfrac{1}{2}\rangle\}\\&\times|ij;[11]\rangle.\end{aligned} \tag{9}$$

Therefore, the use of the size parameters c_i and d_j, which are $c_i\neq\sqrt{4/3}d_j$, is important to have the other flavor-spin symmetries and to produce the different behaviors between the pairs, namely, diquarklike correlations. In the case of the *s* wave, the size parameters with $c_i\neq\sqrt{4/3}d_j$ produce $[21]_o$ and enable us to take $[21]_{fs}$ into consideration. For the *p* wave, the size parameters with $c_i\neq\sqrt{4/3}d_j$ produce the orbital part of $[3]_o$ and $[111]_o$, which couple to $[3]_{fs}$ and $[111]_{fs}$, respectively.

B. Matrix element

Employing a variational principle, we obtain the following equation to get the eigenvalues E and eigenvectors χ:

$$H\chi=EN\chi, \tag{10}$$

where the Hamiltonian and normalization matrices H and N are given by

$$\begin{aligned}H&=\langle i,j,M_fS|H\mathcal{S}|i',j',M_f'S'\rangle,\\N&=\langle i,j,M_fS|\mathcal{S}|i',j',M_f'S'\rangle.\end{aligned} \tag{11}$$

Here we have abbreviated $|ij;[o]\rangle|M_f;(S,\frac{1}{2})s\rangle$ to $|i,j,M_fS\rangle$. The eigenvector χ is normalized in the following way:

$$\chi^\dagger N\chi=\sum_{ijM_fSi'j'M_f'S'}C_{ijM_fS}\langle i,j,M_fS|\mathcal{S}|i',j',M_f'S'\rangle\times C_{i'j'M_f'S'}=1. \tag{12}$$

Due to the symmetrization operator $\mathcal{S}$ in Eq. (3), there are five different types of diagrams corresponding to the following terms. They are for the one-body operators h_i,

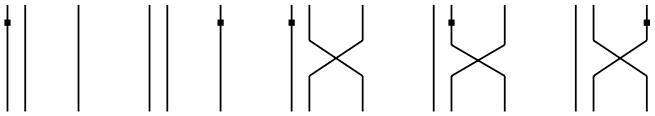

FIG. 1. Five different diagrams for one-body operators. Solid lines are quarks, and dots indicate the one-body operator.

$$h_1, \quad h_3, \quad h_1P_{23}, \quad h_2P_{23}, \quad h_3P_{23},$$

and for the two-body operators v_{ij},

$$v_{12}, \quad v_{23}, \quad v_{12}P_{23}, \quad v_{13}P_{23}, \quad v_{23}P_{23}.$$

They are shown in Figs. 1 and 2. Because there is a diagram where the particles 1 and 3 are exchanged, we have two terms corresponding to diagrams (c)–(e) in both Figs. 1 and 2. There are also two terms corresponding to diagram (a) ($h_1 \rightarrow h_2$) in Fig. 1 and (b) ($v_{23} \rightarrow v_{13}$) in Fig. 2.

III. HAMILTONIAN

In the previous paper [10], various kinds of the chiral and hybrid quark models, which contain one gluon and σ meson exchange potentials, are investigated. Total Hamiltonian is given by

$$H = T + V. \tag{13}$$

The kinetic energy part is treated in the relativistic way [7] or nonrelativistic way,

$$T = \sum_i \sqrt{\boldsymbol{p}_i^2 + m_i^2} \tag{14}$$

or

$$\sum_i \frac{\boldsymbol{p}_i^2}{2m_i} + m_i$$

with c.m. momentum $\boldsymbol{P} = 0$. The potential part consists of a linear confinement, ps meson and σ meson exchange potentials and OGEP,

$$V = \sum_{i>j} -\boldsymbol{\lambda}_i \cdot \boldsymbol{\lambda}_j a_c r_{ij} + V_{ij}^{ps} + V_{ij}^{\sigma} + V_{ij}^{OGEP}, \tag{15}$$

where the color factor is $\langle \boldsymbol{\lambda}_i \cdot \boldsymbol{\lambda}_j \rangle = -8/3$ for a color singlet three-quark system. In this paper, we consider the chiral quark model, so OGEP will not be included.

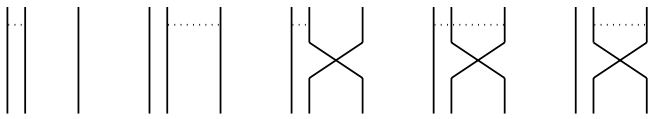

FIG. 2. Five different diagrams for two-body operators. Solid lines are quarks, and dotted lines indicate the two-body interaction.

The ps meson exchange part V_{ij}^{ps} contains the SU(3) octet mesons, namely, π, K, η, and SU(3) singlet meson η' exchange potentials with the following form:

$$V_{ij}^{ps} = \frac{1}{3}\frac{g^2}{4\pi}\frac{m_{ps}^2}{4m_i m_j} \boldsymbol{f}_i \cdot \boldsymbol{f}_j \boldsymbol{\sigma}_i \cdot \boldsymbol{\sigma}_j \left\{ \frac{e^{-m_{ps} r_{ij}}}{r_{ij}} - \left(\frac{\Lambda_{ps}}{m_{ps}}\right)^2 \frac{e^{-\Lambda_{ps} r_{ij}}}{r_{ij}} \right\}, \tag{16}$$

where g is the quark-meson coupling constant, $\boldsymbol{f}$ and $\boldsymbol{\sigma}$ are flavor U(3) generators ($f^{(0)} = \sqrt{2/3}$) and Pauli spin operators, respectively. The form factor Λ_{ps} appears because the quarks are dressed, which prevents the collapse due to the attractive δ function potential, and Λ_{ps} is assumed to depend on the ps meson mass m_{ps} and the flavor-independent parameter Λ_0 in the following way [6]:

$$\Lambda_{ps} = \Lambda_0 + \kappa m_{ps}. \tag{17}$$

The quark-meson coupling constants are $g = g_8$ for π, K and η, and $g = g_0$ for η' meson.

For the analysis of the p-wave states, we also include the following tensor term of the ps meson exchange potential:

$$V_{tensij}^{ps} = \frac{1}{3}\frac{g^2}{4\pi}\frac{m_{ps}^3}{4m_i m_j} \boldsymbol{f}_i \cdot \boldsymbol{f}_j S_{ij} \left\{ H(m_{ps} r_{ij}) - \left(\frac{\Lambda_{ps}}{m_{ps}}\right)^3 H(\Lambda_{ps} r_{ij}) \right\}, \tag{18}$$

where

$$H(x) = \left(1 + \frac{3}{x} + \frac{3}{x^2}\right)\frac{e^{-x}}{x} \tag{19}$$

and

$$S_{12} = 3\boldsymbol{\sigma}_1 \cdot \hat{\boldsymbol{\rho}} \boldsymbol{\sigma}_2 \cdot \hat{\boldsymbol{\rho}} - \boldsymbol{\sigma}_1 \cdot \boldsymbol{\sigma}_2, \quad \hat{\boldsymbol{\rho}} = \frac{\boldsymbol{\rho}}{\rho}. \tag{20}$$

This term contributes to the mass difference between the spin states, $s = \frac{1}{2}$ and $s = \frac{3}{2}$, and mixes these two states for a given j state. We explain how to calculate the tensor term in the Appendix.

The chiral partner of the ps mesons is the σ meson, whose exchange potential is given by

$$V_{ij}^{\sigma} = -\frac{g_8^2}{4\pi}\left(\frac{e^{-m_\sigma r_{ij}}}{r_{ij}} - \frac{e^{-\Lambda_\sigma r_{ij}}}{r_{ij}}\right). \tag{21}$$

The coupling constant is taken to be the same as that for the octet ps mesons. We also introduce the form factor for the σ meson exchange potential, which is given by the same formula used for the ps meson exchange potential in the chiral quark model [see Eq. (17)]. Note that the ps and σ meson exchange potentials we use here has the nonrelativistic form.

IV. CALCULATION OF MATRIX ELEMENTS

The SU(3) octet ps meson exchange potential in Eq. (16) has the $\boldsymbol{f}_i \cdot \boldsymbol{f}_j \boldsymbol{\sigma}_i \cdot \boldsymbol{\sigma}_j$ flavor-spin-dependent short range attrac-

TABLE I. Matrix elements of flavor-spin operators.

$[f]_f$	$[f]_s$	$[f]_{fs}$	FF	SS	X
[3]	[3]	[3]	4	3	4
[3]	[21]	[21]	4	−3	−4
[21]	[3]	[21]	−2	3	−2
[21]	[21]	[3]	−2	−3	14
[21]	[21]	[21]	−2	−3	2
[21]	[21]	[111]	−2	−3	−10
[111]	[3]	[111]	−8	3	−8
[111]	[21]	[21]	−8	−3	8

tion. Employing the following matrix elements,

$$\begin{aligned}
\langle [2]_F | \boldsymbol{f}_1 \cdot \boldsymbol{f}_2 | [2]_F \rangle &= \tfrac{4}{3}, \\
\langle [11]_F | \boldsymbol{f}_1 \cdot \boldsymbol{f}_2 | [11]_F \rangle &= -\tfrac{8}{3}, \\
\langle S=1 | \boldsymbol{\sigma}_1 \cdot \boldsymbol{\sigma}_2 | S=1 \rangle &= 1, \\
\langle S=0 | \boldsymbol{\sigma}_1 \cdot \boldsymbol{\sigma}_2 | S=0 \rangle &= -3,
\end{aligned} \tag{22}$$

we expect that a distance between two quarks in a pair with flavor symmetry $[F]=[11]$ and spin $S=0$ becomes small to gain a short range attraction. Therefore the most interesting point is the behavior of the pairs with the flavor-spin $([F]S)=([11]0)$. In order to discuss this point, we calculate the expectation value of the number of pairs $([F]S)$ and the mean distance of two quarks in the pairs.

First we introduce a projection operator $P_{ij}^{([F])}$ and $P_{ij}^{(S)}$ for the ith and jth quarks, which are given by

$$P_{ij}^{([2])} = \frac{8+3\boldsymbol{f}_i \cdot \boldsymbol{f}_j}{12}, \quad P_{ij}^{([11])} = \frac{4-3\boldsymbol{f}_i \cdot \boldsymbol{f}_j}{12}, \tag{23}$$

$$P_{ij}^{(S=1)} = \frac{3+\boldsymbol{\sigma}_i \cdot \boldsymbol{\sigma}_j}{4}, \quad P_{ij}^{(S=0)} = \frac{1-\boldsymbol{\sigma}_i \cdot \boldsymbol{\sigma}_j}{4}. \tag{24}$$

Then the number of pairs with $([F]S)$ in the octet baryon is given by

$$\hat{N}_{([F]S)} = \sum_{i>j} P_{ij}^{([F])} P_{ij}^{(S)}. \tag{25}$$

In Table I, the following flavor, spin, and flavor-spin matrix elements for their symmetries $[f]$ are given:

$$SS = \left\langle \sum_{i>j} \boldsymbol{\sigma}_i \cdot \boldsymbol{\sigma}_j \right\rangle,$$

$$FF = \left\langle \sum_{i>j} \boldsymbol{f}_i \cdot \boldsymbol{f}_j \right\rangle,$$

$$X = \left\langle \sum_{i>j} \boldsymbol{f}_i \cdot \boldsymbol{f}_j \boldsymbol{\sigma}_i \cdot \boldsymbol{\sigma}_j \right\rangle.$$

Note that the following is the Casimir operator for SU(6):

$$C = \frac{2}{3} SS + FF + X = \begin{cases} 10 & \text{for } [3]_{fs} \\ -2 & \text{for } [21]_{fs} \\ -14 & \text{for } [111]_{fs}. \end{cases}$$

Employing the matrix elements in the table, we obtain, for example, for the SU(3) octet $[21]_f$ baryons with $s=\frac{1}{2}$ $([21]_s)$,

$$N_{([11]0)} = N_{([2]1)} = \frac{10+X}{16}, \quad N_{([11]1)} = N_{([2]0)} = \frac{14-X}{16}. \tag{26}$$

The value X for a flavor-spin SU(6) symmetry enables us to obtain some information how the three quarks in the baryon couple with each other. For the octet and $s=\frac{1}{2}$ baryons, the value X is written as

$$14 n_{[3]_{fs}} + 2 n_{[21]_{fs}} - 10 n_{[111]_{fs}} = X, \tag{27}$$

where $n_{[f]_{fs}}$ is the mixing probability of three-quark $[f]_{fs}$ state in the octet baryon. In the case of our calculation for *s*-wave octet baryons, $[111]_o$ is not taken into account, which means $n_{[111]_{fs}}=0$, then the mixing probability of $[21]_{fs}$ symmetry in the octet baryon is given by

$$n_{[21]_{fs}} = \frac{14-X}{12} = \frac{4}{3} N_{([11]1)}. \tag{28}$$

The formula in Eq. (26) tells that the number of pairs with the flavor and spin $([F]S)=([2]1)$ and $([11]0)$ are the same in the octet baryon and it is impossible to increase only the number of pairs with $([F]S)=([11]0)$. However, their behaviors can be different from each other. In order to discuss this point, we introduce the following operator to calculate a distance between two quarks in the pair $([F]S)$:

$$\hat{O}_{([F]S)} = \sum_{i>j} P_{ij}^{([F])} P_{ij}^{(S)} (\boldsymbol{r}_i - \boldsymbol{r}_j)^2. \tag{29}$$

Then the distance between two quarks in the pair $([F]S)$ is given by dividing the above expectation value by the number of pairs in the following way:

$$\sqrt{r^2_{pair([F]S)}} = \sqrt{\frac{O_{([F]S)}}{N_{([F]S)}}}. \tag{30}$$

V. RESULT

A. Analysis of chiral quark model

We first perform a calculation employing the chiral quark model. We have employed the chiral quark model parameters used by Glozman *et al.* [6] for *s*-wave SU(3) baryons in Ref. [10] to check whether the method of our model works to describe the SU(3) baryons. There the kinetic energy part is taken to be a relativistic form and the ps octet meson exchange potentials are employed. In addition, the singlet η' meson exchange potential that suppresses the short range at-

TABLE II. Parameters of Graz group semirelativistic chiral quark model [6].

Quark and meson mass (MeV)					
m_u, m_d	m_s	m_π	m_K	m_η	$m_{\eta'}$
340	500	139	494	547	958
$\frac{g_8^2}{4\pi}$	$(g_0/g_8)^2$	Λ_0 (fm^{-1})	κ	V_0 (MeV)	a_c (MeV/fm)
0.67	1.34	2.87	0.81	−416	172.4

traction is included in order to obtain the stable solution [10]. Then a constant V_0 is added to shift all baryon masses instead of including the attraction due to the OGEP and the σ meson exchange potential. The parameters used in Ref. [6] are given in Table II.

The energy spectra are shown in Figs. 3 and 4 for *s*-wave and in Figs. 5 and 6 for *p*-wave baryons. The contributions of each term are also shown in Table III. They are well fitted to the experimental values. As we have studied before in Ref. [10], our calculational method is based on the eigenvalue problem, so we can calculate some excited states if the model space to solve the three-quark system is wide enough. The results of the present calculation using our model are consistent with the results of the Graz group [6,22,23].

In Table IV, the number of pairs $([F]S)$ and the distance between two quarks of the pair in *s*- and *p*-wave baryons are given. As we have mentioned in the preceding section, the numbers of the pairs $([2],S=1)$ and $([11],S=0)$ are the same. There is, however, a large difference between the distances of the two quarks in the pairs $([2],S=1)$ and $([11],S=0)$. The distance in the pair $([11],S=0)$ is very small due to the strong short range attraction of the ps meson exchange potential, which can be seen in all baryons. The reason why there is no difference between the distances in the pairs $([2],S=0)$ and $([11],S=1)$ of *s*-wave baryons is

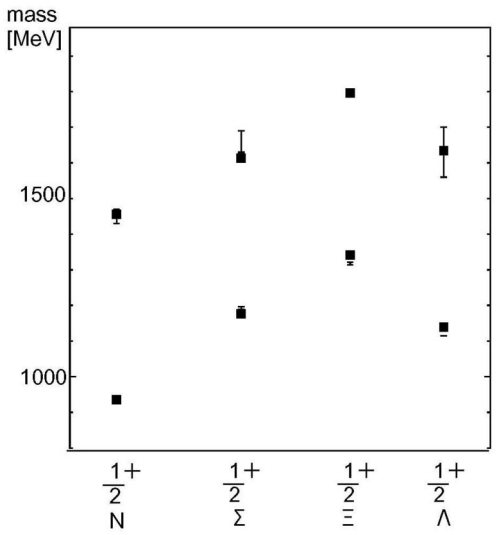

FIG. 3. Energy levels of *s*-wave octet baryons for the set of parameters of Table II. The square corresponds to $s=1/2$. The error bars represent experimental uncertainties.

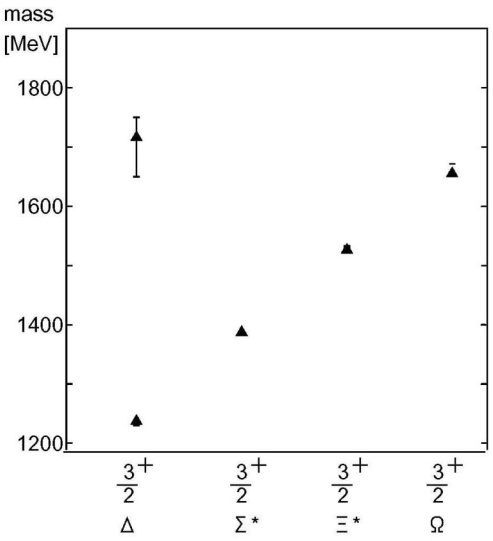

FIG. 4. Energy levels of *s*-wave decuplet baryons for the set of parameters of Table II. The triangle corresponds to $s=3/2$. The error bars represent experimental uncertainties.

that the trial orbital wave function that couples to $([2],S=0)$ and $([11],S=1)$ is not employed explicitly. These states, $([2],S=0)$ and $([11],S=1)$, can appear in the treatment of exchange terms where there is no difference between the orbital parts that couple to these two flavor-spin states.

In the *p*-wave nucleon $N^*(p$ wave), the number of pairs $([2],S=1)$ and $([11],S=0)$ are slightly larger than that of $([2],S=0)$ and $([11],S=1)$ because of the mixing of flavor-spin symmetries other than $[21]_{fs}$. It must be also noted that the distance in the pair $([11],S=0)$ is much shorter than others. In the case of *p*-wave baryons, the radial wave function that couples to $([2],S=0)$ and $([11],S=1)$ is

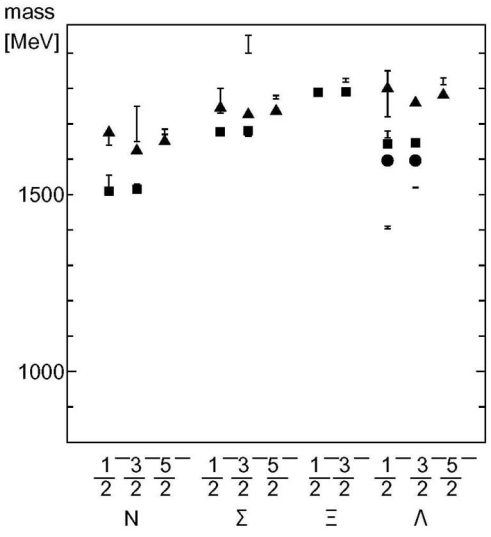

FIG. 5. Energy levels of *p*-wave octet and singlet baryons for the set of parameters of Table II. The square corresponds to $s=1/2$, and the triangle corresponds to $s=3/2$, and the circle corresponds to flavor singlet Λ with $s=1/2$. The error bars represent experimental uncertainties.

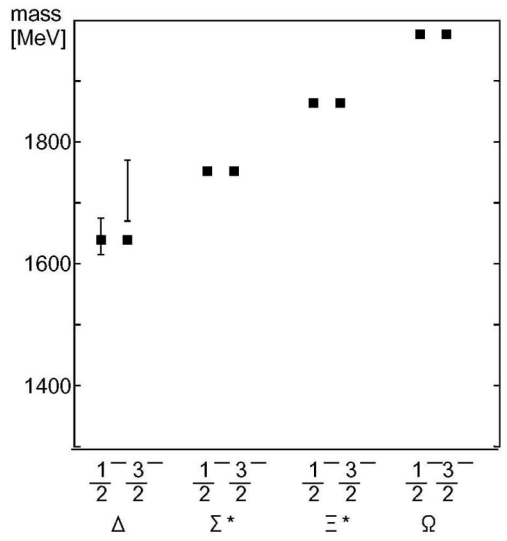

FIG. 6. Energy levels of *p*-wave decuplet baryons for the set of parameters of Table II. The square corresponds to $s=1/2$. The error bars represent experimental uncertainties.

used explicitly. So their sizes can be different from each other.

This chiral quark model has been well analyzed for *s*-wave baryons in Ref. [10], and we made some comments on this chiral quark model. First, we found that the contribution from the pion exchange potential to the mass difference between nucleon and Δ, which is 889 MeV in the chiral quark model, and that is much larger than the observed value 293 MeV. Second, in order to obtain the correct mass, the constant $3V_0=-1248$ MeV was added, and this negative constant stands for the attraction coming from the σ meson exchange or the gluonic effects. However, when we include more realistic form for the attraction, such as the σ meson exchange potential or OGEP, the solution becomes unstable and almost collapse. Finally, the inclusion of the SU(3) singlet ps meson η' was also necessary to obtain the stable solution in the semirelativistic approach.

Here we make some comments on the new analysis including the *p*-wave baryons. In this model, the energy spectra agree well with the experimental values even for the excited states including the Roper resonance. This is a nice

TABLE III. Results for octet and decuplet baryons using the Graz group chiral quark model parameters. These blanks in the EXP mean the vanishing experimental states.

Baryon		EXP	M	T	V_{conf}	V_π	V_K	V_η	$V_{\eta'}$	V_{ten}	$\sqrt{r^2}$ (fm)
N	$j=\frac{1}{2}$	938	936	2307	630	−987	0	74	160	0	0.304
Roper	$j=\frac{1}{2}$	1440^{+30}_{-10}	1456	2463	931	−925	0	72	163	0	0.464
$N^*(p$ wave)	$j=\frac{1}{2}$	1535^{+20}_{-15}	1509	1986	1033	−352	0	34	70	−14	0.437
$N^*(p$ wave)	$j=\frac{3}{2}$	1520^{+10}_{-5}	1515	1979	1039	−360	0	35	72	−24	0.438
$N^*(p$ wave)	$j=\frac{1}{2}$	1650^{+30}_{-10}	1675	1801	1142	−32	0	−8	−13	30	0.498
$N^*(p$ wave)	$j=\frac{3}{2}$	1700^{+50}_{-50}	1624	1831	1107	−20	0	−9	−16	−21	0.503
$N^*(p$ wave)	$j=\frac{5}{2}$	1675^{+10}_{-5}	1650	1811	1126	−19	0	−9	−16	5	0.499
Σ	$j=\frac{1}{2}$	1193^{+4}_{-4}	1177	2889	598	−75	−984	−321	318	0	0.299
$\Sigma(p$ wave)	$j=\frac{1}{2}$		1678	2140	1020	−4	−228	−75	81	−8	0.446
$\Sigma(p$ wave)	$j=\frac{3}{2}$	1670^{+15}_{-5}	1681	2137	1024	−4	−234	−77	84	−1	0.448
$\Sigma(p$ wave)	$j=\frac{1}{2}$	1750^{+50}_{-20}	1745	1947	1094	−23	−21	−5	−11	12	0.491
$\Sigma(p$ wave)	$j=\frac{3}{2}$		1726	1962	1075	−24	−14	−3	−14	−8	0.497
$\Sigma(p$ wave)	$j=\frac{5}{2}$	1775^{+5}_{-5}	1736	1848	1088	−24	−13	−2	−15	2	0.493
Ξ	$j=\frac{1}{2}$	1318^{+3}_{-3}	1342	2615	653	0	−693	−238	253	0	0.317
$\Xi(p$ wave)	$j=\frac{1}{2}$		1789	2276	1000	0	−244	−82	92	2	0.440
$\Xi(p$ wave)	$j=\frac{3}{2}$	1820^{+5}_{-5}	1791	2273	1002	0	−246	−82	93	−1	0.440
Λ	$j=\frac{1}{2}$	1115	1139	2333	659	−596	−230	51	170	0	0.318
$\Lambda(p$ wave)	$j=\frac{1}{2}$	1670^{+10}_{-10}	1643	2108	1018	−244	−70	13	74	−8	0.443
$\Lambda(p$ wave)	$j=\frac{3}{2}$	1690^{+5}_{-5}	1646	2105	1020	−249	−70	13	76	−1	0.443
$\Lambda(p$ wave)	$j=\frac{1}{2}$	1800^{+50}_{-80}	1800	1917	1131	5	−36	11	−6	26	0.504
$\Lambda(p$ wave)	$j=\frac{3}{2}$		1759	1945	1101	11	−36	11	−8	−17	0.506
$\Lambda(p$ wave)	$j=\frac{5}{2}$	1830^{+0}_{-20}	1781	1927	1119	12	−35	11	−9	4	0.506
$\Lambda(p$ wave)	$j=\frac{1}{2},\frac{3}{2}$	1407^{+113}_{-4}	1596	2213	962	−215	−206	−43	133	0	0.413
Δ	$j=\frac{1}{2}$	1232^{+2}_{-2}	1237	1836	829	−98	0	−28	−54	0	0.390
$\Delta(p$ wave)	$j=\frac{1}{2},\frac{3}{2}$	1620^{+150}_{-5}	1639	1817	1120	−19	0	−10	−21	0	0.498
Σ^*	$j=\frac{1}{2}$	1385	1387	1908	844	−29	−67	13	−34	0	0.398
Ξ^*	$j=\frac{3}{2}$	1530	1526	1997	852	0	−59	6	−22	0	0.399
Ω	$j=\frac{3}{2}$	1672	1655	2101	852	0	0	−35	−15	0	0.395

TABLE IV. Number of pairs ($[F]S$) and the distance between two quarks of the pair in octet baryons.

	($[F]S$)	([11],0)	([2],1)	([2],0)	([11],1)
N	$N_{([F]S)}$	1.490	1.490	0.010	0.010
$j=\frac{1}{2}$	$\sqrt{r^2_{pair([F]S)}}$ (fm)	0.500	0.549	0.736	0.736
Roper	$N_{([F]S)}$	1.472	1.472	0.028	0.028
$j=\frac{1}{2}$	$\sqrt{r^2_{pair([F]S)}}$ (fm)	0.732	0.860	1.08	1.08
$N^*(p$ wave)	$N_{([F]S)}$	0.773	0.773	0.727	0.727
$j=\frac{1}{2}$	$\sqrt{r^2_{pair([F]S)}}$ (fm)	0.555	0.824	0.964	0.926
Σ	$N_{([F]S)}$	1.483	1.483	0.017	0.017
$j=\frac{1}{2}$	$\sqrt{r^2_{pair([F]S)}}$ (fm)	0.481	0.538	0.639	0.639
$\Sigma(p$ wave)	$N_{([F]S)}$	0.760	0.760	0.740	0.740
$j=\frac{1}{2}$	$\sqrt{r^2_{pair([F]S)}}$ (fm)	0.577	0.794	0.944	0.914

feature of this model. There are various quark models that are helpful for us to understand the structure of the low lying baryons. One of the famous constituent quark models including the study of excited baryons is the nonrelativistic quark model of Isgur and Karl [2], where the main part of the residual interaction is the OGEP. However, they had a difficulty in getting the proper mass spectrum of the Roper resonance. The ordering of the mass spectra of the nucleon and its excited states are the s-wave $N(938)$, s-wave Roper resonance $N^*(1440)$, and the p-wave nucleons $N^*(1520)$ and $N^*(1535)$. They are different from those of the harmonic oscillator model, where the mass of the Roper resonance $N^*(1440)$ must be larger than the p-wave resonances $N^*(1520)$ and $N^*(1535)$ by $\hbar\omega$. Although we use the semirelativistic kinetic term and the linear confinement potential, the orderings of the excited states are roughly the same as the harmonic oscillator states if the residual interaction is weak. Therefore the energy of the Roper resonance is higher than that of the p-wave resonances. To reproduce the masses of these resonances properly, there must be some strong attractive contributions coming from the residual interaction to lower the mass of the Roper resonance. In the chiral model, such contributions come from the flavor-spin dependent ps meson exchange potential and the relativistic treatment of the kinetic energy.

The dominant part of the ps meson exchange potential at short distances has the following form:

$$V^{ps} \sim \sum_{i>j} -\boldsymbol{f}_i \cdot \boldsymbol{f}_j \boldsymbol{\sigma}_i \cdot \boldsymbol{\sigma}_j \delta(r_{ij}). \tag{31}$$

How to calculate the expectation value for $\boldsymbol{f}_i \cdot \boldsymbol{f}_j \boldsymbol{\sigma}_i \cdot \boldsymbol{\sigma}_j$ for a flavor-spin SU(6) symmetry is shown in Sec. IV. Because the nucleon $N(938)$ and the Roper resonance mainly consist of $[3]_{fs}$ and the p-wave resonances mainly consist of $[21]_{fs}$, the Roper resonance ($X=14$) gains the stronger attraction than the p-wave resonances ($X=2$). The relativistic approach on the kinetic energy part is also important. The relativistic kinetic energy $\sqrt{p^2+m^2}-m$ increases more gradually than that of the nonrelativistic form $p^2/2m$ as the momentum p increases. Therefore the contribution of the short range attractive ps meson exchange potential in the semirelativistic approach works more effectively than that of the nonrelativistic one. So in the semirelativistic approach, it becomes much easier to make the mass of the Roper resonance lower than that of the p-wave nucleons due to ps mesons exchange potential. It must be noted that the contribution from the pion exchange potential to the mass difference between the p-wave nucleons and the Roper resonance becomes about 560 MeV. In this way the chiral quark model with the relativistic form of the kinetic energy can reproduce the mass spectra of the baryons quite nicely.

We also give a comment on the tensor term. As you see in Table III, the contribution from the tensor term is very small and the calculated mass spectra are within the error bar of the observed values. This is because the tensor term does not contribute to the $s=\frac{1}{2}$ state but contributes only to the $s=\frac{3}{2}$ state and to the mixing between $s=\frac{1}{2}$ and $s=\frac{3}{2}$ (Appendix). These small values are favorable for explaining the observed values.

On the other hand, the mass ordering between $j=\frac{1}{2}$ and $j=\frac{3}{2}$ states of N^* is different from the observed one. The calculation of Ref. [8] also failed to explain the observed mass ordering with the chiral potential. Therefore we can say that the tensor term of the ps meson exchange potential does not work effectively to fit the mass ordering of negative parity states. We note that these mass differences cannot be fitted with an LS term from confinement potential because the mass ordering of $j=\frac{1}{2}$ and $\frac{3}{2}$ states of the lower part is different from that of the upper part. Of course the observed error bar is so large that this discrepancy about the mass ordering is not necessarily taken seriously.

Now we show the mixing amplitudes in Table V. These mixing amplitudes are very small compared with the results of other groups, such as those of Ref. [8]. These differences are due to the different treatments to describe the baryons. In their calculation, they only focus on the p-wave states, and they use only the symmetries of the potential and baryon states for fitting the parameters. They do not take into account the dynamical behavior of the orbital wave function. However, in our model we have tried to reproduce the mass

TABLE V. Mixing amplitude for octet *p*-wave baryons for the set of parameters of Table II.

Baryon		M	$^4 8$	$^2 8$
N	$j=\frac{1}{2}$	1509	0.205	0.979
	$j=\frac{1}{2}$	1675	0.978	−0.209
	$j=\frac{3}{2}$	1516	−0.098	0.995
	$j=\frac{3}{2}$	1624	0.995	0.099
Σ	$j=\frac{1}{2}$	1678	0.225	0.974
	$j=\frac{1}{2}$	1745	0.974	−0.227
	$j=\frac{3}{2}$	1681	−0.103	0.995
	$j=\frac{3}{2}$	1726	0.995	0.103
Ξ	$j=\frac{1}{2}$	1789	0.138	0.990
	$j=\frac{3}{2}$	1791	−0.055	0.999
Λ	$j=\frac{1}{2}$	1643	0.159	0.987
	$j=\frac{1}{2}$	1800	0.987	−0.161
	$j=\frac{3}{2}$	1646	−0.07	0.997
	$j=\frac{3}{2}$	1759	0.997	0.07

spectra of *s*- and *p*-wave baryons simultaneously and also taken into account the dynamics of the quark wave function explicitly.

As we have mentioned above, the contribution from the ps meson exchange is very large for the *s*-wave octet baryons and the size of the nucleon becomes very small such as 0.3 fm. The short range attraction of the one ps meson exchange potential is due to the δ function smeared by the cutoff parameter Λ_{ps} in Eq. (16). Note that this attraction strongly depends on the cutoff parameter Λ_{ps}, especially in the case of the semirelativistic calculation.

B. Nonrelativistic quark model

In the preceding section we have learned the importance of the ps meson exchange potential in order to explain the baryon spectra. As we have pointed out, the relativistic form of the kinetic energy is also an important factor to lower the mass of the Roper resonance. However, the ps meson exchange potential used in the semirelativistic approach has a nonrelativistic form. It may be consistent to employ the nonrelativistic expression of the kinetic energy term when we use the nonrelativistic form of the ps meson exchange potential. Then we replace the kinetic energy term by the nonrelativistic form, and we also change the parameters of the Graz group's chiral model and reproduce the mass spectra of the SU(3) baryons including excited states, especially we pay attention to the mass of the Roper resonance. The parameters we used in the nonrelativistic calculation are summarized in Table VI. For the sake of simplicity we do not take into account the tensor term here. The results that reproduce the spectra of the Roper resonance and *p*-wave baryons are given in Table VII.

As we have mentioned before, $-\boldsymbol{f}_i\cdot\boldsymbol{f}_j\boldsymbol{\sigma}_i\cdot\boldsymbol{\sigma}_j\delta(r_{ij})$ term of the ps meson exchange potential plays a role to lower the mass of the Roper resonance. However, the nonrelativistic kinetic term suppresses the short range part of the relative wave function strongly, so the contribution of the short range attraction due to the ps meson exchange potential becomes smaller than that of the semirelativistic calculation. Then in order to lower the mass of the Roper resonance, we need a larger coupling constant and cutoff parameter than those of the previous Graz group's model.

TABLE VI. Parameters of the nonrelativistic chiral quark model.

Quark and meson mass (MeV)					
m_u, m_d	m_s	m_π	m_K	m_η	$m_{\eta'}$
330	404	139	494	547	958
$\frac{g_8^2}{4\pi}$	$(g_0/g_8)^2$	Λ_0 (fm^{-1})	κ	V_0 (MeV)	a_c (MeV/fm)
0.85	2.3	8.23	1.3	−173.7	70

As seen in Table VII, the contribution of the pion exchange potential V_π in $N(938)$ becomes -2343 MeV. This is much larger than Graz group's one -987 MeV or the observed mass of the nucleon 938 MeV. It is doubtful to introduce such a large attraction V_π. Because of this strong attraction, the size of nucleon ($\sim$0.38 fm) is smaller than other nonrelativistic models in Ref. [10] ($\sim$0.6 fm) and is similar to the semirelativistic Graz group's one ($\sim$0.3 fm). In addition to that, this solution is in a delicate balance between strong attraction and repulsion, so its solution becomes unstable against a slight change of these potential parameters. It seems hard to justify this solution, even though we can fit the mass spectra of the baryons including the Roper resonance numerically in the nonrelativistic calculation.

C. Modified semirelativistic quark model

In this section, we first show a difference between the nonrelativistic and relativistic kinetic energies at short distances. Furthermore we compare the difference with the magnitude of the ps meson exchange potential at short distances. For this purpose, we evaluate the matrix elements of these operators by the $0s$ harmonic oscillator wave function with a size parameter b. The results are shown in Fig. 7 as a function of b. As seen in the figure, the difference between the nonrelativistic and relativistic kinetic energies are quite large for a small b value. The difference is as large as the contributions from the short range attraction due to the ps meson exchange potential. Because the replacement of the nonrelativistic kinetic energy by the relativistic one causes the large difference at short distances, the short range attractive part due to the meson exchange potential must be reinvestigated by including some relativistic effects, which weaken the strong short range attraction in the semirelativistic approach.

Now we propose another semirelativistic quark model by improving the short range part.

From the analyses of the quark models in the preceding sections, we have learned the following points. The observed mass spectrum suggests that the ps meson exchange potential, whose attraction works more strongly in the Roper resonance $[3]_{fs}$ than in the *p*-wave nucleons $[21]_{fs}$, is favorable.

TABLE VII. Results of the nonrelativistic quark model for octet and decuplet baryons.

Baryon		EXP	M	T	V_{conf}	V_π	V_K	V_η	$V_{\eta'}$	$\sqrt{r^2}$ (fm)
N	$j=\frac{1}{2}$	938	939	3102	319	−2343	0	98	284	0.384
Roper	$j=\frac{1}{2}$	1440^{+30}_{-10}	1452	2224	669	−1169	0	60	189	0.793
$N^*(p$ wave)	$j=\frac{1}{2}$	1535^{+20}_{-15}	1504	1728	687	−582	0	44	148	0.679
Σ	$j=\frac{1}{2}$	1193^{+4}_{-4}	1193	3191	343	−204	−1740	−532	656	0.420
Ξ	$j=\frac{1}{2}$	1318^{+3}_{-3}	1316	2617	383	0	−1283	−475	595	0.461
Λ	$j=\frac{1}{2}$	1115	1133	2709	353	−1231	−714	157	380	0.425

To include the pion exchange between quarks, we take the framework of the chiral quark model. It is well known that the scalar meson σ is a chiral partner of the pseudoscalar mesons. The flavor singlet η' meson is not included, at least originally, in the framework. Thus, we should include the σ meson exchange potential explicitly, rather than a mere constant, and remove the η' meson from a basic model. Its effect, as well as the effects from other mesons, such as vector mesons, may be included in more finely tuned models. Both of these two points, namely, taking a constant attraction instead of employing the σ meson exchange potential and including the η' meson, have been introduced by the Graz group to make the system stable against the strongly attractive short range part of the pion exchange. Thus, we have to examine especially this short range attraction.

The actual improvement is done as follows. As mentioned before, one has to take into account the relativistic effects on the potentials when the relativistic kinetic energy is employed. One of the most important relativistic effects is the energy dependence, which weakens the potential at short distances. For example, in the pion exchange, $1/4m_i m_j$ in Eq. (16) should be replaced by $1/4E^2$. This can be effectively taken into account up to the order q^2 by modifying Λ_π as

$$\frac{\Lambda_{rel}^2 \Lambda_\pi^2}{(\Lambda_{rel})^2 + \Lambda_\pi^2}, \tag{32}$$

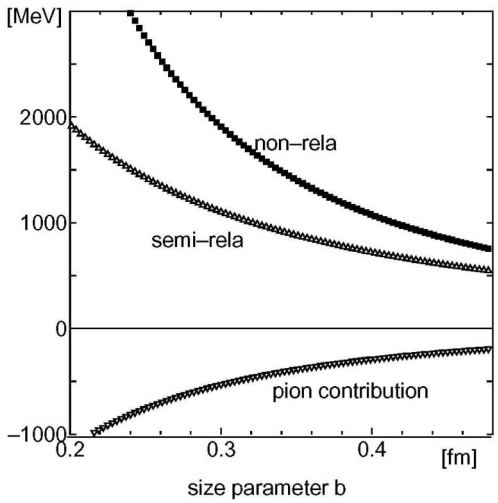

FIG. 7. The diagonal matrix elements of the semirelativistic and nonrelativistic kinetic energy and pion exchange potential. The parameters are the same used in the Graz model.

with a newly introduced cutoff parameter Λ_{rel}. After this modification, the value of Λ_π decreases, for example, from 4.0 fm^{-1} to $\sim$2.5 fm^{-1} with the simplest estimation $\Lambda_{rel} = 2m_q$. This modification may be too simple to discuss the problem quantitatively, but one can argue that the cutoff parameter tends to decrease due to the relativistic effect. According to this argument, we employ the cutoff parameters that are smaller than those used in other models [24]. The parameters are given in Table VIII.

The cutoff parameter for π meson exchange potential $\Lambda_\pi = \Lambda_0 + \kappa m_\pi = 2.46$ fm^{-1} is smaller than that of other models, $\Lambda_\pi = 3.44$ fm^{-1} in Ref. [6] or the generally used value $\Lambda_\pi \sim 4.0$ fm^{-1}. This cutoff parameter makes the solution for the baryons stable even if the σ meson exchange potential is explicitly included. Furthermore, we do not need to include the η' meson exchange potential to prevent the collapse of the solution. It seems still necessary to include the constant attraction V_o, though it becomes somewhat smaller. We have found that the constant attraction is not needed in the model with the weak confinement [10], which cannot produce the mass difference between the *s*- and *p*-wave nucleons. This may suggest that the additional attraction comes from the change of the vacuum or the nonperturbative effects, which we do not discuss here. Obtained energy spectra are shown in Figs. 8–11.

These spectra are in good agreement with the observed masses of the SU(3) baryons. However, the mass of the flavor singlet $\Lambda(1405)$ is not reproduced, similarly as the Graz group model has failed. The results for the *s*-wave ground states, the Roper resonance and the *p*-wave resonances are shown in Table IX. The contribution of the π meson exchange potential becomes smaller than that of the Graz group model, although its value looks still large. It must be noted that the size of the Roper resonance is close to that of *p*-wave nucleon due to the strong attraction for the Roper resonance. It must also be noted that the contribution from the σ meson

TABLE VIII. Parameters of the modified semirelativistic chiral quark model.

Quark and meson mass (MeV)					
m_u, m_d	m_s	m_π	m_K	m_η	m_σ
313	530	139	494	547	675
$\frac{g_8^2}{4\pi}$	$(g_0/g_8)^2$	Λ_0 (fm^{-1})	κ	V_0 (MeV)	a_c (MeV/fm)
0.69	0	1.81	0.92	−378.3	170

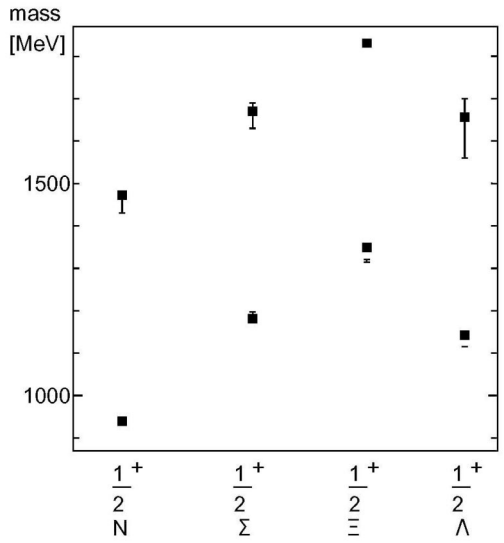

FIG. 8. Energy levels of *s*-wave octet baryons for the set of parameters of Table VIII. The square corresponds to $s=1/2$. The error bars represent experimental uncertainties.

exchange potential to the mass difference between the Roper resonance and the *p*-wave nucleon is 44 MeV, which is comparable to the observed difference 75 MeV. Therefore the σ meson exchange potential also plays a role to lower the mass of the Roper resonance, even though the σ exchange potential is flavor-spin independent. This is because the orbital part of the relative wave function of the Roper resonance is well localized at short distances. As seen in Eq. (21), the σ exchange potential is a short range attraction with the cutoff parameter. The contribution of this potential is strongly influenced by the behavior of the wave function at short distances. In order to see the difference between the relative wave function in the baryons, we calculate

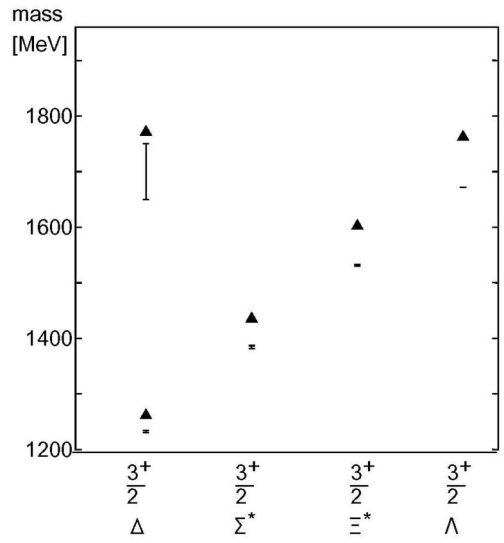

FIG. 9. Energy levels of *s*-wave decuplet baryons for the set of parameters of Table VIII. The triangle corresponds to $s=3/2$. The error bars represent experimental uncertainties.

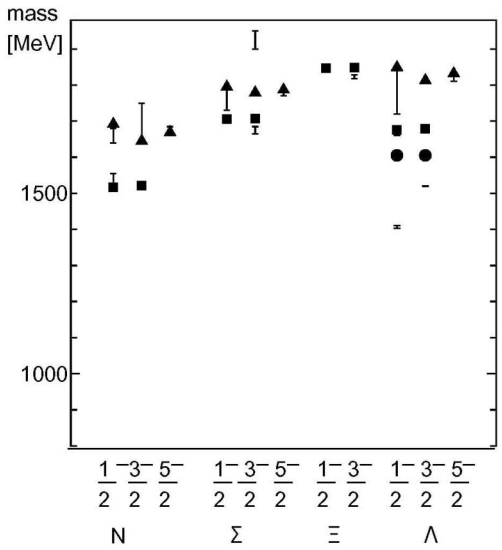

FIG. 10. Energy levels of *p*-wave octet and singlet baryons for the set of parameters of Table VIII. The square corresponds to $s=1/2$, and the triangle corresponds to $s=3/2$, and the circle corresponds to flavor singlet Λ with $s=1/2$. The error bars represent experimental uncertainties.

$$\chi(r)=\langle \boldsymbol{\rho},\boldsymbol{\lambda}|\,\delta(\rho-r)\,|\boldsymbol{\rho},\boldsymbol{\lambda}\rangle, \tag{33}$$

where $|\boldsymbol{\rho},\boldsymbol{\lambda}\rangle=\Phi(\boldsymbol{\rho},\boldsymbol{\lambda})$ are the nucleon and their resonance states. They are shown in Fig. 12. From this figure, we can see the well localized wave function of the Roper resonance at short distances, which is similar to that of the pure harmonic-oscillator model. Therefore the short-ranged σ exchange potential gives stronger attraction for the Roper resonance than the *p*-wave nucleon even though this potential does not depend on the flavor-spin.

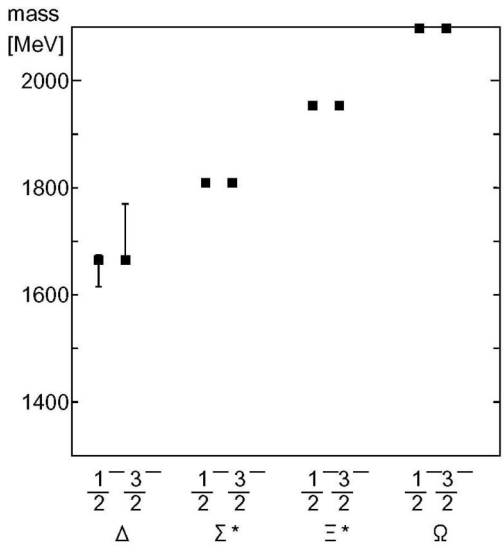

FIG. 11. Energy levels of *p*-wave decuplet baryons for the set of parameters of Table VIII. The square corresponds to $s=1/2$. The error bars represent experimental uncertainties.

TABLE IX. Results of modified semirelativistic chiral quark model for octet and decuplet baryons. These blanks in the EXP means the vanishing experimental states.

Baryon		EXP	M	T	V_{conf}	V_π	V_K	V_η	V_σ	V_{ten}	$\sqrt{r^2}$ (fm)
N	$j=\frac{1}{2}$	938	938	2296	629	−798	0	90	−144	0	0.307
Roper	$j=\frac{1}{2}$	1440^{+30}_{-10}	1473	2442	924	−729	0	86	−115	0	0.468
$N^*(p$ wave)	$j=\frac{1}{2}$	1535^{+20}_{-15}	1517	2019	1001	−334	0	46	−71	−9	0.431
$N^*(p$ wave)	$j=\frac{3}{2}$	1520^{+10}_{-5}	1521	2018	1004	−340	0	47	−71	−2	0.431
$N^*(p$ wave)	$j=\frac{1}{2}$	1650^{+30}_{-10}	1691	1742	1126	−16	0	−5	−50	29	0.506
$N^*(p$ wave)	$j=\frac{3}{2}$	1700^{+50}_{-50}	1645	1771	1093	−7	0	−6	−52	−19	0.509
$N^*(p$ wave)	$j=\frac{5}{2}$	1675^{+10}_{-5}	1669	1751	1112	−6	0	−7	−51	5	0.507
Σ	$j=\frac{1}{2}$	1193^{+4}_{-4}	1182	2905	593	−35	−735	−249	−162	0	0.301
$\Sigma(p$ wave)	$j=\frac{1}{2}$		1706	2285	969	0	−249	−84	−77	−3	0.429
$\Sigma(p$ wave)	$j=\frac{3}{2}$	1670^{+15}_{-5}	1707	2285	970	1	−252	−85	−76	∼0	0.429
$\Sigma(p$ wave)	$j=\frac{1}{2}$	1750^{+50}_{-20}	1795	1935	1069	−17	−11	−3	−54	11	0.496
$\Sigma(p$ wave)	$j=\frac{3}{2}$		1777	1950	1052	−18	−7	−2	−56	−7	0.500
$\Sigma(p$ wave)	$j=\frac{5}{2}$	1775^{+5}_{-5}	1787	1938	1064	−18	−7	−2	−55	2	0.498
Ξ	$j=\frac{1}{2}$	1318^{+3}_{-3}	1349	3049	583	0	−732	−253	−163	0	0.290
$\Xi(p$ wave)	$j=\frac{1}{2}$		1847	2479	934	0	−260	−89	−80	−2	0.416
$\Xi(p$ wave)	$j=\frac{3}{2}$	1820^{+5}_{-5}	1848	2479	935	0	−262	−89	−80	∼0	0.417
Λ	$j=\frac{1}{2}$	1115	1143	2511	618	−552	−205	54	−148	0	0.306
$\Lambda(p$ wave)	$j=\frac{1}{2}$	1670^{+10}_{-10}	1676	2216	969	−242	−69	17	−74	−6	0.432
$\Lambda(p$ wave)	$j=\frac{3}{2}$	1690^{+5}_{-5}	1679	2216	970	−245	−69	17	−74	−1	0.432
$\Lambda(p$ wave)	$j=\frac{1}{2}$	1800^{+50}_{-80}	1849	1924	1098	8	−25	8	−52	23	0.506
$\Lambda(p$ wave)	$j=\frac{3}{2}$		1812	1950	1071	13	−25	8	−54	−16	0.506
$\Lambda(p$ wave)	$j=\frac{5}{2}$	1830^{+0}_{-20}	1832	1932	1087	13	−24	8	−53	4	0.507
$\Lambda(p$ wave)	$j=\frac{1}{2},\frac{3}{2}$	1407^{+113}_{-4}	1604	2429	893	−216	−232	−46	−89	0	0.391
Δ	$j=\frac{1}{2}$	1232^{+2}_{-2}	1261	1704	853	−59	0	−16	−86	0	0.403
$\Delta(p$ wave)	$j=\frac{1}{2},\frac{3}{2}$	1620^{+150}_{-5}	1665	1751	1112	−6	0	−6	−51	0	0.501
Σ^*	$j=\frac{1}{2},\frac{3}{2}$	1385	1435	1871	839	−20	−40	8	−88	0	0.403
Ξ^*	$j=\frac{1}{2},\frac{3}{2}$	1530	1602	2037	824	0	−41	6	−89	0	0.393
Ω	$j=\frac{1}{2},\frac{3}{2}$	1672	1762	2202	809	0	0	−23	−91	0	0.380

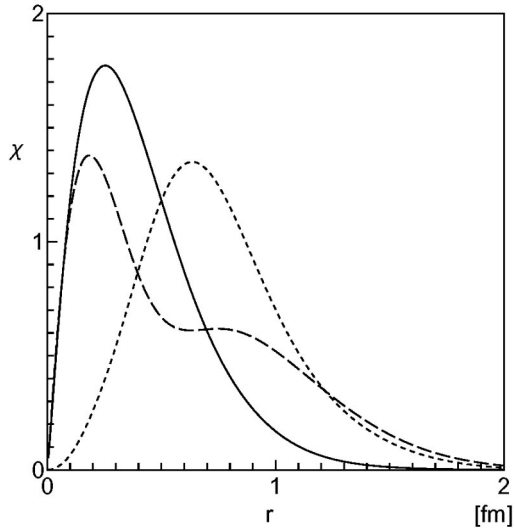

FIG. 12. The behavior $\delta(\rho-r)$ of wave function. The solid line corresponds to ground state nucleon. The dash line corresponds to Roper resonance. The dot line corresponds to p-wave nucleon.

The pion tensor term gives little contribution also in this model because of the same reason as the Graz model. Since the σ exchange potential does not have the tensor term, and the tensor term of the η' meson exchange is found to be small, these two models are not very different from each other as far as the tensor term is concerned. The mass ordering of $j=\frac{1}{2}$ and $\frac{3}{2}$ states is also not reproduced by the present model. Mixing amplitudes in Table X are also similar to the previous results using the Graz model.

Mixing amplitudes of our chiral quark models are smaller than those of Ref. [17], which were empirically obtained from experimental data by using $SU(6)_w$ model. In Ref. [18], Isgur *et al.* showed that the quark model with OGEP gives large mixing amplitude $(-32°)$ for $j=\frac{1}{2}$, which is consistent with the empirical value $(\sim -32°)$. Since this value is much larger than that given by Graz group $(-12°)$, they argued that the OGEP model is superior than the chiral quark model [25]. This difference in size is, however, caused not only by the difference between the interactions but also by the orbital treatment, as explained in the followings.

In the calculation of Ref. [18], they used the single-ranged Gaussian basis for the orbital part, whereas in the calculation

TABLE X. Mixing amplitude for octet *p*-wave baryons of modified chiral quark model.

Baryon		M	$^4 8$	$^2 8$
N	$j=\frac{1}{2}$	1517	0.161	0.987
	$j=\frac{1}{2}$	1692	0.987	−0.163
	$j=\frac{3}{2}$	1522	−0.072	0.997
	$j=\frac{3}{2}$	1645	0.997	0.07
Σ	$j=\frac{1}{2}$	1706	0.132	0.991
	$j=\frac{1}{2}$	1795	0.991	−0.132
	$j=\frac{3}{2}$	1708	−0.05	0.997
	$j=\frac{3}{2}$	1779	0.999	0.053
Ξ	$j=\frac{1}{2}$	1847	0.090	0.996
	$j=\frac{3}{2}$	1848	−0.033	0.999
Λ	$j=\frac{1}{2}$	1676	0.124	0.992
	$j=\frac{1}{2}$	1849	0.992	−0.126
	$j=\frac{3}{2}$	1679	−0.05	0.999
	$j=\frac{3}{2}$	1813	0.999	0.05

by the Graz group the orbital part was given by solving the three quark system. The single-ranged Gaussian calculation with the one-pion exchange potential (OPEP) interaction gives, for example, $-19°$ employing the size parameter $b=0.6$ fm. The above mixing angle is smaller than the OGEP value $-32°$ because the diagonal OPEP tensor part enlarges the separation of the two states given by the spin-spin term, while that of the OGEP tends to cancel the spin-spin part.

Our results with many-ranged Gaussian bases, which are essentially equivalent to the Graz group's calculation, gave much smaller mixing amplitudes: $-20°$ for the OGEP model and $-12°$ for the chiral quark model. This is because the short-ranged central component is enhanced more than the tensor part by solving the orbital wave function. Furthermore, the reduction of the overlap of the upper and lower states also makes the mixing amplitude smaller.

The above results suggest that OGEP produces a larger mixing amplitude than OPEP does. However, it is still difficult for OGEP as well as for OPEP to explain the large empirical mixing in the exactly solved constituent quark model. More complicated processes may contribute to this mixing amplitude. Therefore, the argument that the OGEP model is better than the chiral model because the former can explain the large mixing amplitude is inappropriate. In Ref. [26], for example, the coherent states of pions was introduced to the constituent quark model. They obtained $-43°$ for the mixing angle, which is much larger than without the coherent states, $-24°$. The effect of the meson cloud seems also to contribute to the mixing amplitude considerably though there is still ambiguity in the OPEP parameters and the results may change after taking into account the diquark correlation.

Moreover, the empirical value itself may change. The study for the η photoproduction in Ref. [27] shows that the model, which introduces the third resonance, gives smaller mixing angle ($\sim -26.6°$) than that of $\mathrm{SU}(6)_{\mathrm{w}}$. In their calculation, they introduce a third $S11$ resonance, which is predicted in Ref. [28]. It is considered to be a molecular-type structure, which is not explained by the simple constituent quark model and this state has not been found. This resonance improves the fitting of the ηN decay properties. This picture may be consistent with our result.

Let us make a comment further on OGEP from a viewpoint of the Roper resonance. The hybrid model including OGEP is also one of the interesting quark models. The color magnetic part V_{mag} of OGEP, which has $\boldsymbol{\sigma}_i \cdot \boldsymbol{\sigma}_j v_o$ dependence, becomes $-3v_o$ for the nucleon while it becomes $3v_o$ for Δ, which contains only pairs with $[2]_F$ and $S=1$. This has been believed to explain the mass difference between the nucleon and Δ. In fact in the nonrelativistic hybrid quark model in Ref. [10], a part of the mass difference between the nucleon and Δ is reproduced by OGEP. This is because the ps meson exchange potential alone cannot explain the mass difference between the nucleon and Δ in the nonrelativistic quark model, and this supports the hybrid picture for the baryons. On the other hand, the mass difference between the nucleon and Δ can be reproduced only with the ps meson exchange potential, which is strongly enhanced at short distances in the semirelativistic quark model. This large contribution coming from the ps meson exchange potential plays very important roles to keep the mass of the Roper resonance properly lower than the mass of the *p*-wave nucleons. When we employ OGEP, the contribution of the ps meson exchange potential becomes smaller because a part of the mass difference between the nucleon and Δ is reproduced by OGEP. However, OGEP does not produce the mass difference between the Roper and *p*-wave nucleons so much as the flavor-spin-dependent ps meson exchange potential does. Then it becomes more difficult to fit the mass ordering of the ground state nucleon, the *p*-wave nucleons and the Roper resonance by introducing OGEP. It is possible to make the hybrid model that explain the correct mass ordering of nucleons only when the contribution of OGEP is small enough.

From the analysis of our calculation, we can say that there are three points to reproduce the SU(3) baryons including low-lying excited states, especially the Roper resonance, in the frame work of the present quark models. One is the ps meson exchange potential owning to the flavor-spin-dependent term. Second is the treatment of the relativistic effects, in which the simplest way is the use of the relativistic kinetic energy form. Finally the short range attraction, such as the σ meson exchange potential, can also be the important factor due to the behavior of the wave function at short distances. These clues lead to a nice description of the observed masses of the SU(3) baryons. However, one should not forget that these discussions are based on the assumption that the Roper resonance can be interpreted just as the simple radial excited state of the three-quark system. This interpretation is still in controversy.

VI. SUMMARY

We have performed the study of three-quark system of the SU(3) octet and decuplet baryons employing the extended SU(3) diquarklike cluster model not only for *s*-wave baryons, which we studied in the previous work, but also for *p*-wave baryons. Our diquarklike cluster model enables us to

take into account the mixing of the symmetries other than the usual $[3]_o$ for *s*-wave baryons and $[21]_o$ for *p*-wave baryons. Because of the mixing, the pair in the baryon, which has different flavor-spin quantum numbers, can behave differently. Using the completely antisymmetrized wave function of the baryon, this model can take into account the various symmetries of the states in addition to those assumed in the traditional simple constituent quark model. The number of pairs with a specific symmetry ($[F]S$) and the size of these pairs can also be calculated.

We have improved the diquarklike cluster model in Ref. [10] for the purpose of extending our research to *p*-wave baryons. For *p*-wave baryons, we have employed two types of the orbital wave function. One is the function which is antisymmetric when we exchange quarks 1 and 2, and couples to $[11]_{FS}$. The other function is symmetric under the same exchange, and couples to $[2]_{FS}$. For the more detailed analysis of the chiral quark model, we have taken into account the tensor term. We have found that the tensor term produces small mass differences between the states with $s=\frac{1}{2}$ and $\frac{3}{2}$.

First we have employed the parameters of the chiral quark model proposed by Glozman *et al.* [6], and compared the obtained baryon mass spectra. We found that our calculational method works quite nicely not only for the ground states but also for the excited states in the semirelativistic approach employing the chiral quark model. We also found that the flavor-spin-dependent ps meson exchange potential makes it possible to reproduce the right mass ordering of the nucleon states. Then we have pointed out that the semirelativistic approach works effectively to enhance the ps meson exchange potential in the short range region.

Next, we have employed the nonrelativistic quark model to reproduce the mass spectra as good as the Graz group model. Since the ps meson exchange potential is given in the nonrelativistic form, the nonrelativistic form of the kinetic energy may be consistent. A very strong ps meson-quark coupling constant is, however, needed to obtain the enough attraction to describe the ordering of the Roper and the *p*-wave resonances without a help of the semirelativistic approach. Therefore it is very hard to justify the nonrelativistic approach if we persist in describing the Roper resonance as the radial excitation of the three-quark system.

Then, we have employed the improved semirelativistic chiral quark model, where the chiral partner, the σ meson exchange potential is included in addition to the ps meson exchange potentials. By having introduced the chiral partner σ meson, this effective constituent quark model becomes more suitable to the picture of the chiral symmetry breaking process. The relativistic form of the kinetic energy is, in principle, better than the nonrelativistic one when the potential contains a relativistic correction and the short range part of the potential is well taken care of. In this model, we employ the relativistic form of the kinetic energy and smaller cutoff parameter Λ_{ps}, which simulates a part of the relativistic effects for the potential terms. This means that we take into account the relativistic effects not only on the kinetic energy part but also on the potential part. This small Λ_{ps} suppresses properly the attractive contribution at short distances, which is enhanced strongly due to the relativistic form of the kinetic energy, and enables us to obtain the stable solution even though the additional attraction due to the σ meson exchange potential is included and the repulsion due to the SU(3) singlet η' meson exchange is omitted. Employing this improved semirelativistic chiral quark model, we have succeeded in reproducing the ordering of the ground state baryons, the *p*-wave baryon resonances and the Roper resonance as successfully as the original chiral quark model.

In this calculation, we also investigate the contributions from the tensor term. We found that both chiral and modified quark models give very small mixing amplitudes, which are different from Ref. [17]. We have also shown that OGEP produces small mixing amplitudes in our exact calculation of the three quark model, which is different from Ref. [18]. We must note that the tensor term produces the wrong mass ordering for the excited nucleon states of N^*. The contributions from the tensor term are, however, very small and the calculated masses are still within the observed error bar.

Therefore we conclude that the model that includes only the ps meson and chiral partner σ meson exchange potential with the semirelativistic treatment seems better than other models as far as the baryon mass spectra are concerned. This conclusion is based on the assumption that the Roper resonance is simply the radial excitation of the three-quark system that consists mainly of the $[3]_{fs}$ symmetry. The interpretation of the Roper resonance is, however, still in controversy. Therefore one needs further investigation on other observables than the mass spectra as well as on the nature of the Roper resonance.

ACKNOWLEDGMENTS

This work was supported in part by a Grant-in-Aid for Scientific Research from JSPS (Grant Nos. 11640258, 12640290)

APPENDIX: TENSOR TERM

The tensor term is rewritten as

$$S_{12}=3\boldsymbol{\sigma}_1\cdot\hat{\boldsymbol{\rho}}\boldsymbol{\sigma}_2\cdot\hat{\boldsymbol{\rho}}-\boldsymbol{\sigma}_1\cdot\boldsymbol{\sigma}_2$$
$$=3\sqrt{5}[[\boldsymbol{\sigma}_1\times\boldsymbol{\sigma}_2]^{(2)}\times[\hat{\boldsymbol{\rho}}\times\hat{\boldsymbol{\rho}}]^{(2)}]_0^{(0)}. \quad \text{(A1)}$$

Then the matrix elements are given by

$$\langle jj_z|S_{12}|jj_z\rangle=3\sqrt{5(2j+1)}\begin{Bmatrix} s & l & j \\ s' & l' & j \\ 2 & 2 & 0 \end{Bmatrix}$$
$$\times\langle s'\|[\boldsymbol{\sigma}_1\times\boldsymbol{\sigma}_2]^{(2)}\|s\rangle\langle l'\|[\hat{\boldsymbol{\rho}}\times\hat{\boldsymbol{\rho}}]^{(2)}\|l\rangle. \quad \text{(A2)}$$

Here we have separated spin and orbital parts by using the $9j$ symbol. The spin part is given by

$$\langle (S'\tfrac{1}{2})s'\|[\boldsymbol{\sigma}_1\times\boldsymbol{\sigma}_2]^{(2)}\|(S\tfrac{1}{2})s\rangle$$
$$=(-1)^{1/2+2+S'+s}\sqrt{(2s'+1)(2s+1)}\begin{Bmatrix} s' & 2 & s \\ S & \frac{1}{2} & S' \end{Bmatrix}$$
$$\times\langle S'\|[\boldsymbol{\sigma}_1\times\boldsymbol{\sigma}_2]^{(2)}\|S\rangle. \quad \text{(A3)}$$

The orbital part for the *p*-wave wave function is taken as

$$|(L_\rho L_\lambda)l=1\rangle=\boldsymbol{c}|l=0\rangle,$$

where $|l=0\rangle$ is the *s*-wave wave function and $\boldsymbol{c}$ is

$$\boldsymbol{c}=\hat{\boldsymbol{\rho}} \quad \text{or} \quad \hat{\boldsymbol{\lambda}}.$$

Then the matrix element for the orbital part is given by

$$\langle (L'_\rho L'_\lambda)l'=1\|[\hat{\boldsymbol{\rho}}\times\hat{\boldsymbol{\rho}}]^{(2)}\|(L_\rho L_\lambda)l=1\rangle$$
$$=-\langle l'=0|[[\boldsymbol{c}'\times\boldsymbol{c}]^{(2)}\times[\hat{\boldsymbol{\rho}}\times\hat{\boldsymbol{\rho}}]^{(2)}]_0^{(0)}|l=0\rangle. \quad \text{(A4)}$$

Employing the above formula, we can calculate the tensor matrix elements for the *p* wave in a similar way as the central part for the *s* wave.

[1] F. E. Close, *An Introduction to Quarks and Partons* (Academic, New York, 1988).
[2] N. Isgur and G. Karl, Phys. Rev. D **19**, 2653 (1979); **20**, 1191 (1979).
[3] A. De Rujula, H. Georgi, and S.L. Glashow, Phys. Rev. D **12**, 147 (1975).
[4] S. Sasaki, T. Blum, and S. Ohta, Phys. Rev. D **65**, 074503 (2002).
[5] L.Ya. Glozman and D.O. Riska, Phys. Rep. **268**, 263 (1996).
[6] L.Ya. Glozman, W. Plessas, K. Varga, and R.F. Wagenbrunn, Phys. Rev. D **58**, 094030 (1998).
[7] S. Capstick and N. Isgur, Phys. Rev. D **34**, 2809 (1986).
[8] H. Collins and H. Georgi, Phys. Rev. D **59**, 094010 (1999).
[9] K. Shimizu, Y.B. Dong, and A. Faessler, Nucl. Phys. **A657**, 283 (1999).
[10] M. Furuichi and K. Shimizu, Phys. Rev. C **65**, 025201 (2002).
[11] M. Anselmino, E. Predazzi, S. Ekelin, S. Fredriksson, and D.B. Lichtenberg, Rev. Mod. Phys. **65**, 1199 (1993).
[12] S. Fleck, B. Silvestre-Brac, and J.M. Richard, Phys. Rev. D **38**, 1519 (1988).
[13] O. Krehl, C. Hanhart, S. Krewald, and J. Speth, Phys. Rev. C **62**, 025207 (2000).
[14] P. Stassart, Fl. Stancu, J.M. Richard, and L. Theußl, J. Phys. G **26**, 397 (2000).
[15] M. Oka and K. Yazaki, in *Quarks and Nuclei*, edited by W. Weise (World Scientific, Singapore, 1985), and references therein.
[16] K. Shimizu, Rep. Prog. Phys. **52**, 1 (1989), and references therein.
[17] A.J.G. Hey and P.J. Litchfield, Nucl. Phys. **B95**, 516 (1975).
[18] N. Isgur and G. Karl, Phys. Lett. **72B**, 109 (1977).
[19] B. Silvestre-Brac and C. Gignoux, Phys. Rev. D **32**, 743 (1985).
[20] J.M. Richard, Phys. Rep. **212**, 1 (1992).
[21] C. Roux and B. Silvestre-Brac, Few-Body Syst. **19**, 1 (1995).
[22] L.Ya. Glozman and K. Varga, Phys. Rev. D **61**, 074008 (2000).
[23] L. Ya. Glozman (private communication).
[24] K. Shimizu, S. Takeuchi, and A.J. Buchmann, Prog. Theor. Phys. Suppl. **137**, 43 (2000).
[25] N. Isgur, Phys. Rev. D **62**, 054026 (2000).
[26] M. Morishita and M. Arima, Phys. Rev. C **65**, 045209 (2002).
[27] B. Saghai and Z. Li, Eur. Phys. J. A **11**, 217 (2001).
[28] N. Kaiser, P.B. Siegel, and W. Weise, Phys. Lett. B **362**, 23 (1995).